ARTICLE OPEN

Check for updates

Ginger essential oil prevents NASH progression by blocking the NLRP3 inflammasome and remodeling the gut microbiota-LPS-TLR4 pathway in mice

Suraphan Panyod[1,2,3,12], Wei-Kai Wu[4,5,6,12], Ya-Chi Hsieh[1], Yea-Jing Tseng[1], Sin-Yi Peng[1], Rou-An Chen[1], Huai-Syuan Huang[1], Yi-Hsun Chen[3], Ting-Chin David Shen[7], Chi-Tang Ho[8], Chun-Jen Liu[3,5], Hsiao-Li Chuang[9], Chi-Chang Huang[10], Ming-Shiang Wu[3,5]✉ and Lee-Yan Sheen[1,2,11]✉

BACKGROUND: Diet and gut microbiota contribute to non-alcoholic steatohepatitis (NASH) progression. High-fat diets (HFDs) change gut microbiota compositions, induce gut dysbiosis, and intestinal barrier leakage, which facilitates portal influx of pathogen-associated molecular patterns including lipopolysaccharides (LPS) to the liver and triggers inflammation in NASH. Current therapeutic drugs for NASH have adverse side effects; however, several foods and herbs that exhibit hepatoprotection could be an alternative method to prevent NASH.
METHODS: We investigated ginger essential oil (GEO) against palm oil-containing HFDs in LPS-injected murine NASH model.
RESULTS: GEO reduced plasma alanine aminotransferase levels and hepatic pro-inflammatory cytokine levels; and increased antioxidant catalase, glutathione reductase, and glutathione levels to prevent NASH. GEO alleviated hepatic inflammation through mediated NLR family pyrin domain-containing 3 (NLRP3) inflammasome and LPS/Toll-like receptor four (TLR4) signaling pathways. GEO further increased beneficial bacterial abundance and reduced NASH-associated bacterial abundance.
CONCLUSION: This study demonstrated that GEO prevents NASH progression which is probably associated with the alterations of gut microbiota and inhibition of the LPS/TLR4/NF-κB pathway. Hence, GEO may offer a promising application as a dietary supplement for the prevention of NASH.

Nutrition and Diabetes (2024)14:65 ; https://doi.org/10.1038/s41387-024-00306-1

INTRODUCTION

Non-alcoholic fatty liver disease (NAFLD) stands as the prevailing chronic liver disease on a global scale, encompassing a broad spectrum of liver conditions [1, 2]. Among these, non-alcoholic steatohepatitis (NASH) represents a distinct entity characterized by hepatic steatosis of at least 5%, accompanied by inflammation and ballooned hepatocytes, with or without concurrent hepatic fibrosis [3]. If left untreated, NASH can advance to liver cirrhosis and, ultimately, hepatocellular carcinoma. The concept of the multiple-hit hypothesis recognizes that environmental factors, such as diet, lifestyle, and gut microbiota, can intricately interact with genetic and epigenetic factors, collectively contributing to the development of liver injury [4]. Typically, NAFLD pathogenesis caused by a high-fat diet (HFD) involves increased hepatic fat accumulation, oxidative stress, and inflammatory responses [5]. HFD intake results in the elevation of free fatty acid (FFA) levels and stimulates the expression of sterol regulatory element-binding protein-1c (SREBP1-c)-mediated de novo lipogenesis and 3-hydroxy-3-methyl-glutaryl-CoA reductase (HMGCR)-mediated cholesterol synthesis. Peroxisome proliferator-activated receptor-α (PPARα), which regulates the oxidation of fatty acids, is expressed at lower levels. These factors promote triglyceride and cholesterol accumulation in the liver [6]. Excessive hepatic FFAs lead to the upregulation of the expression of the cytochrome P450 isoform 2E1 (CYP2E1) and enhance the production of reactive oxygen species (ROS) [7]. Various liver antioxidants and enzymes can reduce oxidative stress, such as glutathione (GSH), catalase (CAT), and superoxide dismutase (SOD) [8]. Oxidative stress can also cause chronic hepatic inflammation. Several studies have confirmed the activation of the NOD-, LRR-, and pyrin domain-containing protein 3 (NLRP3) inflammasome (comprising NLRP3, ASC, and pro-caspase-1) in HFD-induced hepatic steatosis, which induces the production of cytokines interleukin (IL)-1β and -18 and leads to hepatic inflammation and cell death [9, 10].

[1]Institute of Food Science and Technology, National Taiwan University, Taipei, Taiwan, ROC. [2]Center for Food and Biomolecules, National Taiwan University, Taipei, Taiwan, ROC. [3]Department of Internal Medicine, College of Medicine, National Taiwan University, Taipei, Taiwan, ROC. [4]Department of Medical Research, National Taiwan University Hospital, Taipei, Taiwan, ROC. [5]Department of Internal Medicine, National Taiwan University Hospital, Taipei, Taiwan, ROC. [6]Bachelor Program of Biotechnology and Food Nutrition, National Taiwan University, Taipei, Taiwan, ROC. [7]Division of Gastroenterology, Perelman School of Medicine, University of Pennsylvania, Philadelphia, PA, USA. [8]Department of Food Science, Rutgers University, New Brunswick, NJ, USA. [9]National Laboratory Animal Center, National Applied Research Laboratories, Taipei, Taiwan, ROC. [10]Graduate Institute of Sports Science, National Taiwan Sport University, Taoyuan City, Taiwan, ROC. [11]National Center for Food Safety Education and Research, National Taiwan University, Taipei, Taiwan, ROC. [12]These authors contributed equally: Suraphan Panyod, Wei-Kai Wu. ✉email: mingshiang@ntu.edu.tw; lysheen@ntu.edu.tw

Received: 9 August 2023 Revised: 17 June 2024 Accepted: 18 June 2024
Published online: 16 August 2024

Diet and gut microbiota interactions play significant roles in the pathogenesis of NASH [11, 12]. Many recent studies have demonstrated that an unhealthy diet characterized by low fiber, high fat, and high sugar content can induce gut microbiota shifts resulting in gut microbiota dysbiosis and intestinal barrier leakage, which facilitates the portal influx of pathogen-associated molecular patterns (PAMPs) (e.g., lipopolysaccharides [LPS] or endotoxins) to the liver [13, 14]. A previous study found that the administration of LPS promoted hepatocarcinogenesis in mice [15]. Gut-derived bacterial products activate several toll-like receptors (TLRs), including TLR4, in different liver cell types, triggering downstream inflammatory responses and cytokine generation to enhance NASH progression [16]. LPS can activate the TLR4 signaling pathway, leading to nuclear factor kappa B (NF-κB) intracellular signal transduction and the production of inflammatory cytokines such as tumor necrosis factor (TNF)-α, IL-6, and IL-1β [17].

Several rodent models for inducing NASH and liver fibrosis have been validated including trans-fat-containing amylin liver NASH (AMLN) [18–20]. Due to the detrimental impact of trans-fats on health, the US Food and Drug Administration (FDA) has implemented regulations prohibiting their use in the food industry [21–23]. Consequently, the trans-fat animal model may not accurately replicate human dietary patterns. The substitution of trans-fat with palm oil in the diet, a palm oil-containing HFD (P-HFD)–Gubra Amylin NASH (GAN) diet in a mouse model previously confirmed that it leads to an identical phenotype to NASH compared to trans-fat-induced NAFLD mice and demonstrates excellent clinical translatability [24, 25]. Recently, we developed a NASH C57BL/6 J mouse model using a P-HFD supplemented with intraperitoneal injections of LPS to simulate gut dysbiosis and endotoxemia. This animal model yielded an equivalent NASH phenotype, intestinal leakage, and endotoxemia, but developed more extra-intestinal microbiota dysbiosis by increasing pathogenic bacteria and reducing beneficial microbiota [26].

Several approaches have been developed for NASH treatment and prevention, including the use of medications. These NASH therapeutic drugs are still being developed and have adverse side effects [27]. Several foods and herbs have exhibited hepatoprotective function, and they can be used to prevent NASH [28]. Our previous studies have demonstrated that a volatile oil from fresh *Zingiber officinale* Roscoe (ginger), or ginger essential oil (GEO), can potentially alleviate hepatic lipid accumulation, oxidative stress, and pro-inflammatory cytokines against HFD-induced NAFLD [6]. GEO exerts antibacterial and antifungal effects [29, 30]. Moreover, GEO ameliorates atherosclerosis in ApoE$^{-/-}$ mice by modulating trimethylamine-N-oxide and gut microbiota [31]. However, the hepatoprotective effects of GEO against NASH and its impact on the gut microbiota, its metabolites, the gut–liver axis, and NLRP3 inflammasome pathway have not yet been determined. Therefore, this study investigated the hepatoprotective effects of GEO through the NLRP3 inflammasome and gut microbiota-LPS-TLR4 pathway using a P-HFD with LPS-induced NASH, endotoxemia, and gut dysbiosis in mouse models.

METHODS

Ginger essential oil extraction and gas chromatography analysis

Ginger was obtained from the Mingjian Township Farmers' Association of Nantou County (Taiwan). Raw aged ginger was washed and sliced into small pieces. Distilled water was added to sliced ginger (1:3) and mixed using a blender. The aged ginger puree was extracted by steam distillation for approximately 6 h. The yellowish GEO was then collected. The GEO was placed in a −20 °C freezer to exclude water content. The unfrozen liquid was collected and repeatedly placed in the freezer until no frozen liquid portion was detected. The yield of the GEO was 0.14% of the raw aged ginger.

Gas chromatography (GC) was used to analyze the constitution of GEO and its primary compound citral (Sigma-Aldrich Corp., MO, USA). GEO constitution was measured using a Thermo Scientific Focus GC equipped with an AI 3000 II autosampler, a flame ionization detector, and a Stabilwax (crossbond Carbowax-PEG, Restek) column (60 m × 0.32 mm; 1 μm) [6, 32]. The GC chromatogram demonstrated that citral is composed of a mixture of geranial and neral geometric isomers. Citral was the main component of GEO, comprising approximately 31% with 18.8% neral and 12.2% geranial isomers (Supplementary Fig. 1).

Animal model

Animal experiments were performed according to the guidelines established by the Institutional Animal Care and Use Committee of National Taiwan University (IACUC) (Approval No: NTU-110-EL-00060). A previous study established a P-HFD with LPS (PL)-induced NASH mouse model in which the severity of gut microbiota dysbiosis was increased compared to P-HFD alone [26]. Six-week-old male C57BL/6 J mice were purchased from Taiwan National Laboratory Animal Center and housed in an alternate light/dark cycle (12 h) room at a temperature of 23 ± 2 °C and relative humidity of 50–70%. After 2 weeks of adaptive feeding, the mice were randomly assigned to five groups ($n = 7$–8/group): ① control diet (Research Diets, Inc., NJ, USA; D12450K); ② P-HFD (Gubra-Amylin NASH (GAN) diet; Research Diets, Inc., NJ, USA; D09100310) + intraperitoneal injections of LPS (500 μg/kg bw/week; LPS from Escherichia coli O55:B5; Sigma-Aldrich; L2880) (PL); ③ PL + a low dose of GEO (12.5 mg/kg bw/day) (PL + GL); ④ PL + a medium dose of GEO (62.5 mg/kg bw/day) (PL + GM); and ⑤ PL + a high dose of GEO (125 mg/kg bw/day) (PL + GH). All mice for each treatment were housed in separate cages ($n = 3$–4 per cage). GEO was administered to the mice through daily oral gavage. The control diet contained fat (10 kcal%) and carbohydrates, principally corn starch. The P-HFD contained 40 kcal% fat, mainly from palm oil; 20% fructose; and 2% cholesterol [24, 25]. The dosages of GEO selected for this study were based on relevant literature and our previous research, which demonstrated its hepatoprotective effects against NAFLD and alcoholic fatty liver disease [6, 32]. The dosage of 12.5 mg/kg bw of GEO was considered as the 1X dose in our current investigation. Higher dosages of 62.5 and 125 mg/kg bw were chosen as the 5X and 10X doses, respectively, to evaluate efficacy across different dosage levels. Body weight and food intake were recorded every week. The mice were sacrificed by carbon dioxide asphyxiation after 12 weeks. Blood was then collected by cardiac punctures using a heparin-coated syringe and transferred to a collection tube. The mice were dissected to extract various specimens. The liver, spleen, kidney, cecum, the visceral, subcutaneous, epididymal white adipose tissue (WAT) (eWAT), inguinal WAT (iWAT), perirenal WAT (pWAT), mesenteric WAT (mWAT), and inguinal subcutaneous white adipose tissue (isWAT), and interscapular brown adipose tissue (iBAT) were harvested, imaged, and weighed after sacrificing the mice. The fecal contents of the colons were collected for DNA sequencing.

Liver histopathological analysis

The largest right lobe of the liver was fixed in 10% neutral formalin. Histopathological analyses were then performed using the formalin-fixed paraffin-embedded (FFPE) method. Hepatic histological scoring was performed by the College of Veterinary Medicine Animal Disease Diagnostic Center (National Chung Hsing University, Taichung, Taiwan). The NAFLD activity score (NAS) was calculated for steatosis, lobular inflammation, and hepatocyte ballooning. Scores of 5–8 were recognized as diagnostic for NASH [33].

Plasma biochemical analyses

Plasma was extracted by centrifuging the blood at 1000 x *g* for 15 min at 4 °C. The biochemical parameters of the plasma, including the levels of total cholesterol, total triglycerides, low-density lipoprotein (LDL), high-density lipoprotein (HDL), aspartate aminotransferase (AST), alanine aminotransferase (ALT), and glucose (TG), were analyzed using a Beckman Colter AU 5800 (Beckman Colter Inc., USA).

Liver antioxidant capacity and inflammation analysis

In brief, 0.1 g of liver and 1 mL of homogenization buffer (8 mM KH_2PO_4, 12 mM K_2HPO_4, 1.5% KCl, pH = 7.4) were homogenized, followed by centrifugation at 10,000 x *g* for 30 min at 4 °C. The supernatant was collected and stored at −80 °C. Liver homogenates were subjected to assays for GSH, glutathione peroxidase (GPx), glutathione reductase (GRd), superoxide dismutase (SOD), and CAT using commercial kits from Cayman Chemical Co. (Ann Arbor, MI, USA). Inflammatory cytokine levels in the liver

were quantified using enzyme-linked immunosorbent assay (ELISA) kits specific for mouse TNF-α, IL-1β, and IL-6 (Invitrogen, USA) [26].

Western blot analysis

Protein (0.1 g) was extracted with 1 mL of cold lysis buffer (comprising 7 M urea, 2 M thiourea, 2% CHAPS, 0.002% bromophenol blue, 60 mM DTT, and a protease and phosphatase inhibitor cocktail), followed by centrifugation at 17500 x *g* for 30 min 4 °C [34]. The supernatants were collected, and the protein concentration was determined using the Bio-Rad protein assay. Sample buffer (comprising 62.5 mM Tris-HCl, 10% glycerol, 2% SDS, and 0.01% bromophenol blue) was added to the protein samples for protein dilution and boiled at 95 °C for 10 min. Sodium dodecyl sulfate-polyacrylamide gel electrophoresis (SDS-PAGE) was performed to separate the proteins, which were then transferred onto polyvinylidene difluoride (PVDF) membranes (Millipore Corp., Bedford, MA, USA). The membranes were blocked with 5% bovine serum albumin in Tris-buffered saline with Tween 20 (TBST) buffer (20 mM Tris-base, 150 mM NaCl, and 0.05% Tween 20) for 1 h and washed three times with TBST buffer for 5 min each. The membranes were incubated overnight at 4 °C with primary antibodies against SREBP-1c, HMGCR, PPARα, CYP2E1, GAPDH (GeneTex, San Antonio, TX, USA), NLRP3, ASC (Abcam, Cambridge, England), Caspase-1 (Santa Cruz Biotechnology, Santa Cruz, CA, USA), TLR4, and NF-κB (Cell Signaling Technology, Beverly, MA, USA). After removing the unbound primary antibodies with TBST buffer, the membranes were incubated with a horseradish peroxidase-conjugated secondary antibody (GeneTex) at room temperature for 2 h, then washed. An enhanced chemiluminescence (ECL) substrate (PerkinElmer Life Sciences, Boston, MA, USA) was added to the membranes to detect the enzyme-conjugated antibodies. The signals were captured using a UVP BioSpectrum AC imaging system (UVP, Upland, CA, USA). Protein expression was quantified by densitometry using the ImageJ software (version 1.47; NIH, Bethesda, MD, USA). The density of each protein band was normalized to that of the control GAPDH protein.

Fecal DNA extraction, 16 S rRNA amplicon sequencing, and sequencing analyses

Mouse fecal samples were removed from the colons during the sacrifices, snap-frozen using liquid N_2, and stored at −80 °C before use. Genomic DNA from the feces was extracted using the QIAmp Power Fecal Pro DNA Kit (QIAGEN, Netherlands) and quantified using a NanoDrop ND-1000 spectrophotometer (Thermo Fisher Scientific). The V3–V4 hypervariable region of the 16 S rRNA gene was amplified using the following primer pair: forward: 5′-TCG TCG GCA GCG TCA GAT GTG TAT AAG AGA CAG CCT ACG GGN GGC WGC AG-3′ and reverse: 5′-GTC TCG TGG GCT CGG AGA TGT GTA TAA GAG ACA GGA CTA CHV GGG TAT CTA ATC C-3′. PCR amplification was carried out in a 25-μL reaction mixture containing 5 ng of DNA template, 0.2 μM of forward and reverse primers, and 12.5 μL of 2× Taq Master Mix (KAPA HiFi HotStart ReadyMix, Roche, Switzerland). The PCR conditions included a cycle at 95 °C for 3 min, followed by 25 cycles at 95 °C for 30 s, 55 °C for 30 s, 72 °C for 30 s, and a final extension at 72 °C for 5 min. The PCR products were visualized using 2% agarose gel electrophoresis. Dual index and Illumina sequencing adapters were joined via PCR using a Nextera XT Index Kit. PCR product cleanup was performed using AMPure XP beads to purify the amplicons. The sizes of the PCR products were confirmed using a Bioanalyzer DNA 1000 Chip. Library quantification was performed for quality control before sequencing using the Agilent Technologies 2100 Bioanalyzer. Pooled libraries were subjected to paired-end sequencing (2 × 300 bp) using the Illumina MiSeq platform. Raw sequences were processed according to the QIIME2 pipeline [35]. Demultiplexed sequences from each sample were quality filtered and trimmed, de-noised, and merged. The chimeric sequences were then identified and removed using the QIIME2 dada2 plugin. The QIIME2 feature-classifier plugin was then used to align amplicon sequence variant (ASV) sequences against the SILVA database (version 132). The vegan package in R was used to calculate the alpha diversity, including the observed ASVs and Shannon and Simpson indices. A principal coordinate analysis (PCoA) was performed using the Bray–Curtis distance. An analysis of variance (ANOVA) using distance matrices (Adonis) was performed to determine the heterogeneity of fecal microbiota among the groups. A heatmap was plotted using the heatmap3 package in R.

Lipopolysaccharide quantification

Plasma and hepatic LPS levels were quantified using a cell-based colorimetric assay for the detection of biologically active endotoxins. Plasma samples and liver homogenates (10 μL) were added to murine TLR4/NF-κB/secreted embryonic alkaline phosphatase (SEAP) reporter HEK293 cells and incubated for 24 h. After incubation, the medium was removed, and the HEK-Blue™ LPS Detection Kit (InvivoGen, USA) was used to detect TLR4 and an NF-κB-inducible SEAP. The abundances were then measured with a spectrophotometer at 620 nm [26].

Intestinal permeability analysis

Intestinal barrier permeability was examined by gavage with fluorescein isothiocyanate-dextran (FITC-dextran; average molecular weight of 4,000; Sigma-Aldrich, 46944) as an intestinal permeability probe. Fifteen milligrams of FITC-dextran in 0.2 mL of phosphate-buffered saline were gavaged to mice 3 h before sacrifice. Plasma FITC-dextran measurements were taken using a fluorometer at excitation and emission wavelengths of 485 and 538 nm (Fluoroskan Ascent FL, Thermo Fisher Scientific, USA), respectively, in black 96-well plates [36].

Statistical analysis

Data are presented as the mean ± standard deviation (SD). A one-way ANOVA with Dunnett's multiple comparison test was used to compare group means against the PL group. The Wilcoxon signed-rank test, Kruskal–Wallis test with Dunn's multiple comparison test, and ANOVA with Dunnett's multiple comparison test were used to analyze the fecal microbiome dataset. All statistical analyses were performed using GraphPad Prism (version 9.1.2), R (version 3.6.1), or R Studio (version 1.2.5001).

RESULTS

Chemical composition of ginger essential oil

GEO was obtained by steam distillation, and the extraction rate was approximately 0.14% (w/w). The gas chromatography (GC) analysis revealed that the GEO contained 18.8% neral and 12.2% geranial isomers (Supplementary Fig. 1). Both neral and geranial isomers are geometric isomers of citral. Our results, therefore, confirmed that citral is the main component of GEO (approximately 31%). It was subsequently used for the animal studies.

Palm oil-containing HFD with LPS injection resulted in an adverse effect on obesogenic and metabolic biomarkers. Supplementation of GEO ameliorate lipidemia

The experimental design of this study is shown in Fig. 1a. Eight-week-old C57BL/6 mice ($n = 7$–8 per group) were fed a control diet or P-HFD with LPS injection (PL) with or without GEO supplementation via oral gavage. In this study, we supplemented the mice daily with 12.5 (GL), 62.5 (GM), and 125 (GH) mg/kg for 12 weeks. The mice were sacrificed after 12 weeks to investigate the effect of GEO on the prevention of obesogenic, metabolic, and hepatic changes. The PL group exhibited an increased body weight compared to the control (CON) group ($p = 0.0155$) (Fig. 1b). We calculated the weight gain rate based on the increase in body weight and time of feeding; the weight gain rate of the PL group was similar to the body weights, which were higher than those of the CON group (Fig. 1c). At 12 weeks, the body weights in the PL group (30.8 ± 2.0) were significantly higher ($p = 0.0028$) than those in the CON group (26.9 ± 0.8) (Fig. 1d). The relative total fat mass of the PL group was found to be heavily increased compared to the control ($p < 0.0001$), up to 195% of the CON group (Fig. 1e). The relative fat mass in different body locations in the PL group was also higher than that in the CON group. This included the mass of the visceral, subcutaneous, epididymal white adipose tissue (WAT) (eWAT), inguinal WAT (iWAT), mesenteric WAT (mWAT), perirenal WAT (pWAT), and inguinal subcutaneous white adipose tissue (isWAT), and interscapular brown adipose tissue (iBAT) (Fig. 1e, Supplementary Fig. 2). GEO supplementation, especially at medium and high doses, reduced body weight changes ($p < 0.0001$) (Fig. 1b) and tended to slightly lower final body weight and area under the curve of body weight (Fig. 1c, d). No significant difference was observed in the average energy

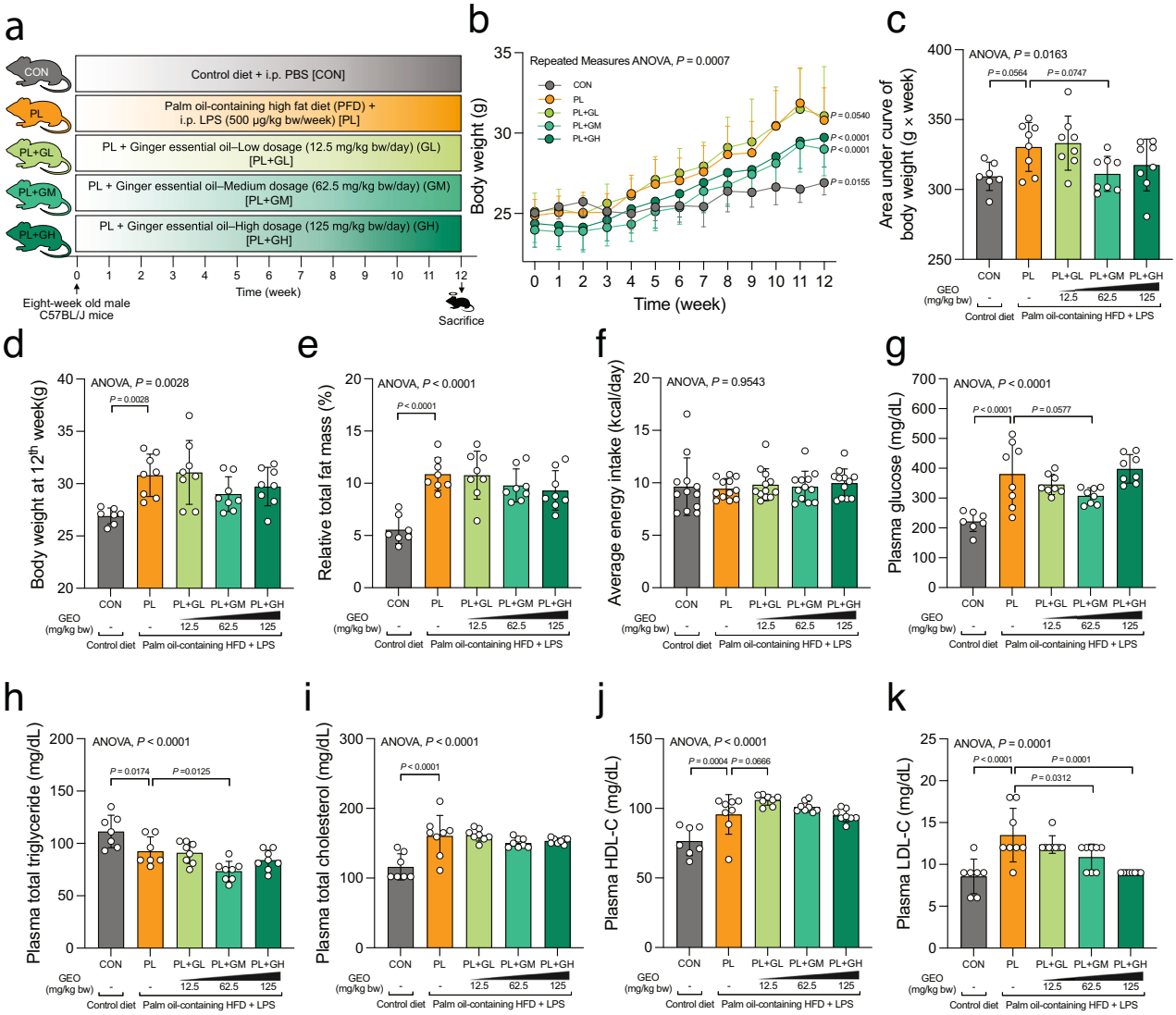

Fig. 1 Palm oil-containing HFD with LPS i.p. (PL) resulted in an adverse effect on obesogenic and metabolic biomarkers. Supplementation with GEO trended to prevent obesity and ameliorated lipidemia. a Experimental design, **b** body weight change, **c** area under the curve of body weight, **d** body weight at 12 weeks, **e** relative total fat mass, **f** average energy intake, **g** plasma glucose, **h** plasma total triglyceride, **i** total cholesterol, **j** high-density lipoprotein (HDL-C), and **k** low-density lipoprotein (LDL-C) in C57BL/6 mice, which were treated with either control or a palm oil-containing HFD with LPS i.p. (PL) with or without ginger essential oil (GEO) (12.5 (GL), 62.5 (GM), and 125 (GH) mg/kg bw) supplementation by daily oral gavage for 12 weeks. Each value was expressed as the mean ± SD ($n = 7–8$). Statistical analyses were performed by repeated measures ANOVA or one-way ANOVA with Dunnett's multiple comparison test for comparing group means against the PL group.

intake among the experimental groups, suggesting that diet type was the primary factor regulating body weight gain (Fig. 1f). The study examined the plasma levels of glucose and lipidemic biomarkers, including fasting glucose, total triglyceride, total cholesterol, high-density lipoprotein cholesterol (HDL-C), and low-density lipoprotein cholesterol (LDL-C) (Fig. 1g–k). Compared to the CON group, the PL group showed significant increases in plasma glucose ($p < 0.0001$), total cholesterol ($p < 0.0001$), HDL-C ($p = 0.0004$), and LDL-C ($p < 0.0001$) levels, indicating the impact of PL on blood fasting glucose and lipid circulation. However, plasma total triglyceride levels were reduced compared to the CON group. Supplementation with GEO at medium dosage reduced plasma glucose ($p = 0.0577$) and total triglyceride ($p = 0.0125$) levels compared to the PL group. Additionally, low-dose GEO trended to improve plasma HDL-C levels ($p = 0.0666$). Both medium and high doses of GEO significantly reduced plasma LDL-C levels ($p = 0.0312$ and $p = 0.0001$, respectively). Collectively, supplementation of GEO, particularly at medium and high doses, significantly improves lipidemia.

GEO prevents NASH with reduced hepatic damage and NAFLD activity scores

AST and ALT are indicators of liver damage. We did not observe an increase in AST levels in the PL group compared to the CON group (Fig. 2a). The plasma ALT levels in the PL group were markedly higher than those in the CON group ($p = 0.0208$) (Fig. 2b). The plasma AST levels trended to be lower in the PL + GM and PL + GH groups. Remarkably, GEO supplementation in the PL + GM and PL + GH groups significantly lowered the ALT levels compared to the PL group ($p = 0.0104$ and $p = 0.0044$, respectively). The liver weight in the PL group exhibited a significant increase compared to the CON group ($p = 0.0006$) (Fig. 2c). However, treatment with GEO did not lead to a reduction in liver weight. The representative image of the liver was shown in Fig. 2d,

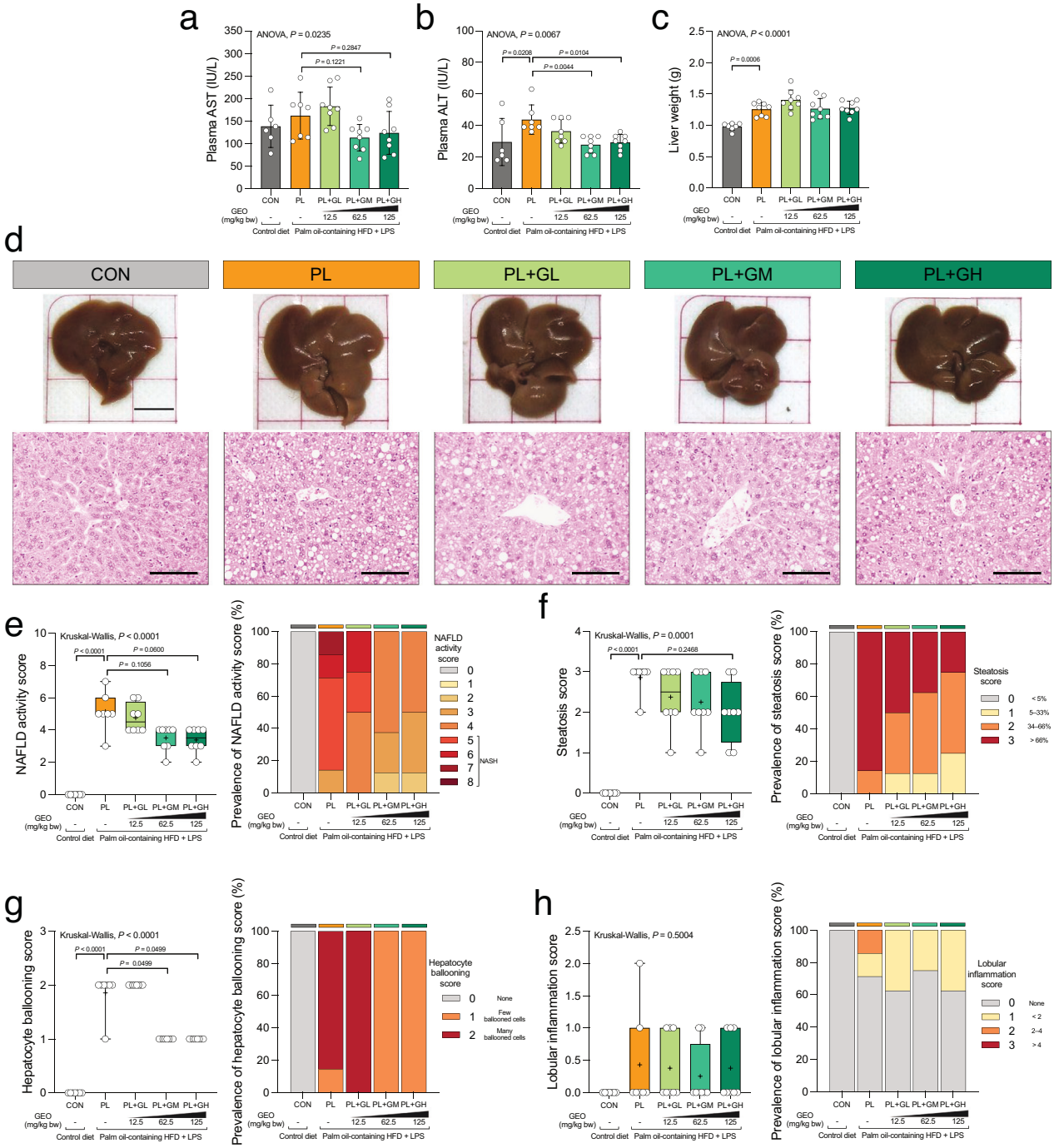

Fig. 2 GEO prevents NASH by improving plasma hepatic damage biomarkers and reversing the NAFLD activity and hepatocyte ballooning scores. a Plasma aspartate aminotransferase (AST), **b** alanine aminotransferase (ALT), **c** liver weight, **d** representative image of liver images (scale bar: 1 cm) and histopathological changes (400X magnification; scale bar: 100 µm), **e** NAFLD activity score, **f** steatosis score, **g** hepatocyte ballooning score, and **h** lobular inflammation score and their prevalence in C57BL/6 mice, which were treated with either control or a palm oil-containing HFD with LPS i.p. (PL) with or without ginger essential oil (GEO) (12.5 (GL), 62.5 (GM), and 125 (GH) mg/kg bw) supplementation by daily oral gavage for 12 weeks. Bar plots were expressed as the mean ± SD ($n = 7–8$). Box plots display median and mean (+), quartiles (boxes), and range (whiskers). Statistical analyses were performed by a one-way ANOVA with Dunnett's multiple comparison test for comparing group means against the PL group.

and hepatomegaly was observed prominently in the PL group. We performed liver histological analyses to determine the impact of PL on NASH progression and the effect of GEO on NASH prevention. Hematoxylin and eosin (H&E) staining of the liver sections showed that the lipid droplets in the PL group were numerous compared to those in the CON group. Based on the NAS, mouse liver sections were examined for steatosis, hepatocyte ballooning, and lobular inflammation scores (Fig. 2d–h). A NAS ≥ 5 was considered to be indicative of NASH. PL induced the NASH phenotype by increasing the NAS (median = 5) compared to the CON group (median = 0) ($p < 0.0001$), resulting in a prevalence of 85.7% for NASH. GEO at low, medium, and high dosages reduced the prevalence of NASH to 50%, 0%, and 0%, respectively, with respective NAS of 4.5, 4, and 3.5. PL-treated mice exhibited

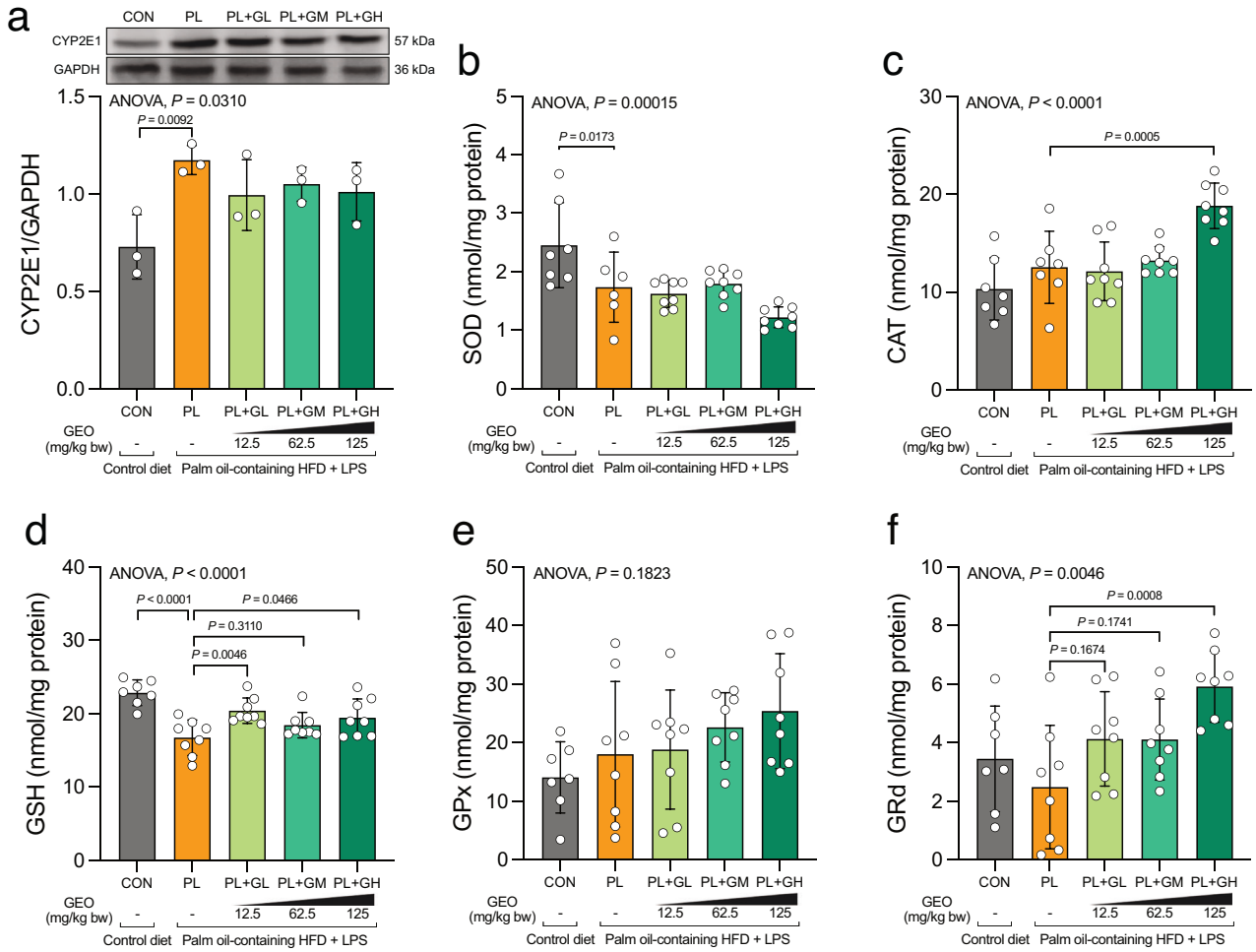

Fig. 3 GEO improves hepatic antioxidant enzyme activities. a Cytochrome P450 2E1 (CYP2E1) protein expression, **b** hepatic superoxide dismutase (SOD), **c** catalase (CAT), **d** glutathione (GSH), **e** glutathione peroxidase (GPx), and **f** glutathione reductase (GRd) in C57BL/6 mice, which were treated with either control or a palm oil-containing HFD with LPS i.p. (PL) with or without ginger essential oil (GEO) (12.5 (GL), 62.5 (GM), and 125 (GH) mg/kg bw) supplementation by daily oral gavage for 12 weeks. Each value was expressed as the mean ± SD ($n = 7–8$). Statistical analyses were performed by a one-way ANOVA with Dunnett's multiple comparison test for comparing group means against the PL group.

increased levels and prevalence of hepatic steatosis, hepatocyte ballooning, and lobular inflammation. GEO exhibited a potential effect on NASH prevention by reversing these scores. The PL + GM and PL + GH groups showed a reduction in the hepatocyte ballooning score compared with the PL group ($p = 0.0499$). Based on the histopathological analysis of liver biopsy results, it was evident that GEO supplementation led to an overall improvement in liver inflammation. The primary mechanism by which GEO reduced the severity of NASH was primarily through the reduction of hepatocyte ballooning. Medium and high doses of GEO were more effective for NASH prevention in PL-treated mice. Overall, these data suggest that GEO can potentially prevent NASH.

GEO improves hepatic antioxidant enzyme activities

A HFD increases fat uptake, and excess fat can accumulate in the liver by increasing ROS and lipid peroxidation, which further causes liver cell damage. Several hepatic antioxidants and enzymes have been found to eliminate ROS. CYP2E1 further increases hepatic oxidative stress. Our data revealed that the PL group exhibited increased CYP2E1 protein expression (Fig. 3a). GEO supplementation trended to reduce CYP2E1 expression. In NASH patients, impaired glutathione metabolism and reduced enzyme activities in the blood support a consistent role of free radical cytotoxicity in the pathophysiology of the disease [37]. PL resulted in the reduction of SOD and GSH levels. Interestingly, GEO supplementation enhanced CAT, GSH, and GRd levels. GPx trended to increase in the GEO-supplemented group (Fig. 3b–f). The overall antioxidant capacity of a high dose of GEO (GH) was more beneficial than that of low and medium doses of GEO. GEO may, therefore, suppress oxidative stress in PL-induced NASH by improving antioxidant and antioxidant enzyme activities.

GEO decreases hepatic inflammation by suppressing pro-inflammatory cytokines and mediating the NLRP3/ACS/caspase-1 pathway

According to the histopathological analysis of the liver biopsy results, GEO alleviated the NAS mainly by reversing steatosis and the hepatocyte ballooning score. We measured the levels of hepatic pro-inflammatory cytokines. PL induced an increase in TNF-α, IL-1β, and IL-6 levels. GEO at medium and high doses significantly reduced hepatic IL-1β ($p = 0.0013$ and $p < 0.0001$, respectively) and IL-6 levels ($p < 0.0001$ and $p < 0.0001$, respectively). In addition, a high dose of GEO significantly decreased TNF-α levels ($p = 0.0012$) (Fig. 4a–c). To investigate the role of GEO in hepatic fatty acid synthesis and β-oxidation, we measured SREBP-1, PPARα, and HMGCR protein expression. PL increased SREBP-1 and HMGCR levels. GEO further favored the reduction of these biomarkers. An increase in PPARα expression was also

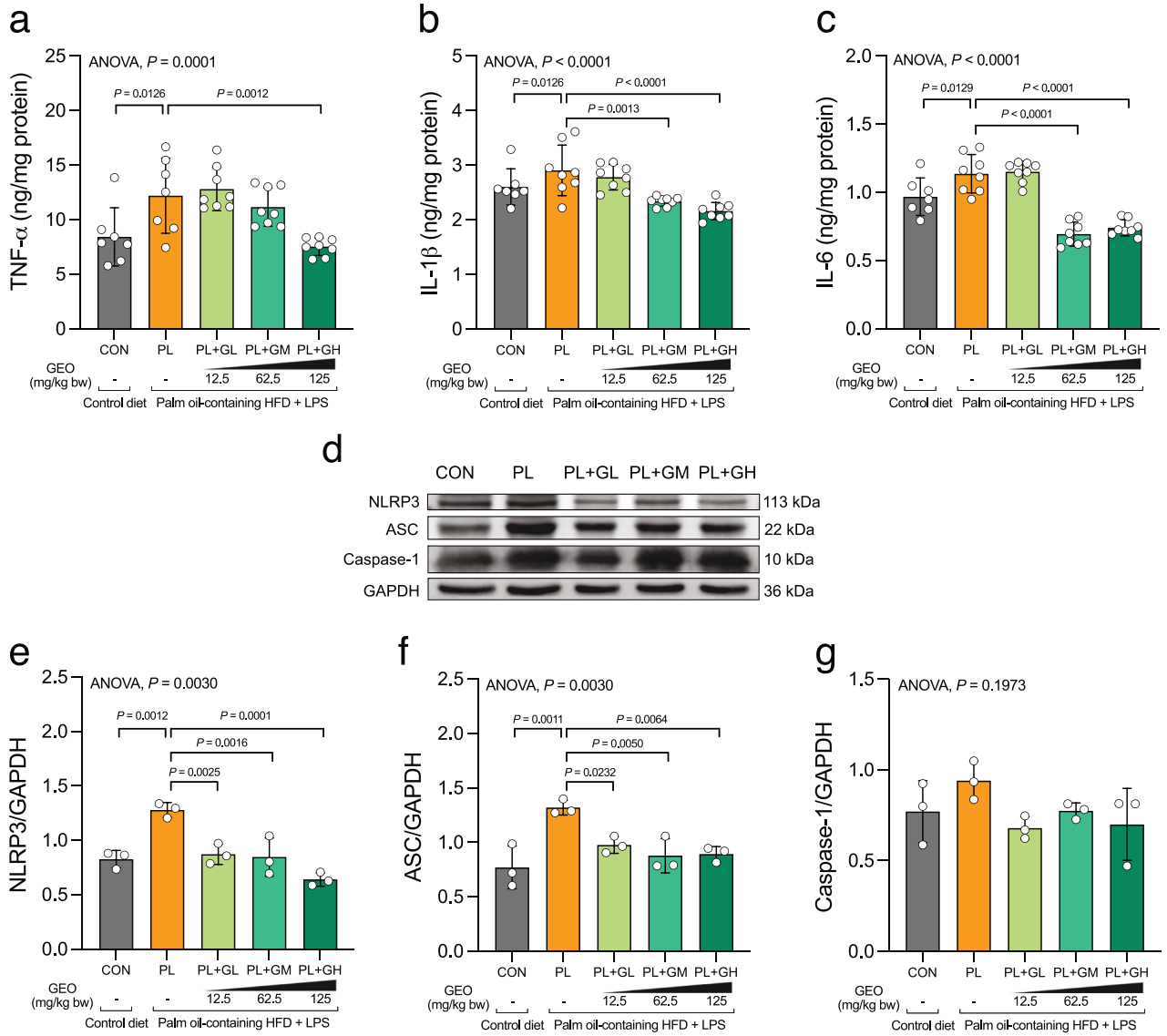

Fig. 4 GEO reduces hepatic inflammation by suppressing inflammatory cytokines and the NLRP3/ASC pathways. a Liver TNF-α, **b** IL-1β, **c** IL-6, **d** representative image of NLRP3, ASC, caspase-1 protein expression, **e** NLRP3, **f** ASC, and **g** caspase-1 in C57BL/6 mice, which were treated with either control or a palm oil-containing HFD with LPS i.p. (PL) with or without ginger essential oil (GEO) (12.5 (GL), 62.5 (GM), and 125 (GH) mg/kg bw) supplementation by daily oral gavage for 12 weeks. Each value was expressed as the mean ± SD ($n = 7–8$), protein expression ($n = 3$). Statistical analyses were performed by a one-way ANOVA with Dunnett's multiple comparison test for comparing group means against the PL group.

observed in the GEO supplemented group (Supplementary Fig. 3). Although the hepatic lipid regulation-related protein expression did not show a significant difference, alteration trends were observed, suggesting that GEO partially exerts a beneficial effect against fatty synthesis and lipid oxidation to prevent NASH. Several studies have further suggested that the NLRP3 inflammasome plays a crucial role in NASH progression. Therefore, we investigated the expression of NLRP3 and its downstream proteins in the liver. The hepatic NLRP3, ACS, and caspase-1 protein levels are shown in Fig. 4d. PL intervention for 12 weeks induced an increase in hepatic NLRP3 and ASC expression compared to control mice ($p = 0.0012$ and $p = 0.0011$, respectively) (Fig. 4e–f). All doses of GEO significantly suppressed NLRP3 and ASC protein expression compared to the PL group ($p < 0.05$). In addition, the hepatic protein expression of caspase-1 trended to increase in the PL group, but was reduced in the GEO-supplemented group (Fig. 4g). These results suggest that GEO mediates the NLRP3/ASC/caspase-1 pathway, resulting in the reduction of pro-inflammatory cytokine production to prevent NASH.

PL and GEO remodel the fecal microbiota composition, and GEO reverses gut microbiota dysbiosis that may benefit NASH amelioration

The gut microbiota plays an important role in the pathogenesis of NASH and its metabolites. To understand the effect of PL and GEO, we sequenced the gene encoding the bacterial V3–V4 16 S rRNA amplicons obtained from feces sampled from the colon. The amplicon sequence variant (ASV) table was generated using the QIIME2 pipeline against the SILVA database (version 132). A total of 1093 ASVs were obtained and assigned to taxonomies at the species level (140 species). We calculated the α-diversity based on the observed ASVs and Shannon and Simpson indices from the ASV table. The observed ASV of the PL group trended to decrease, but the Shannon and Simpson diversity indices significantly

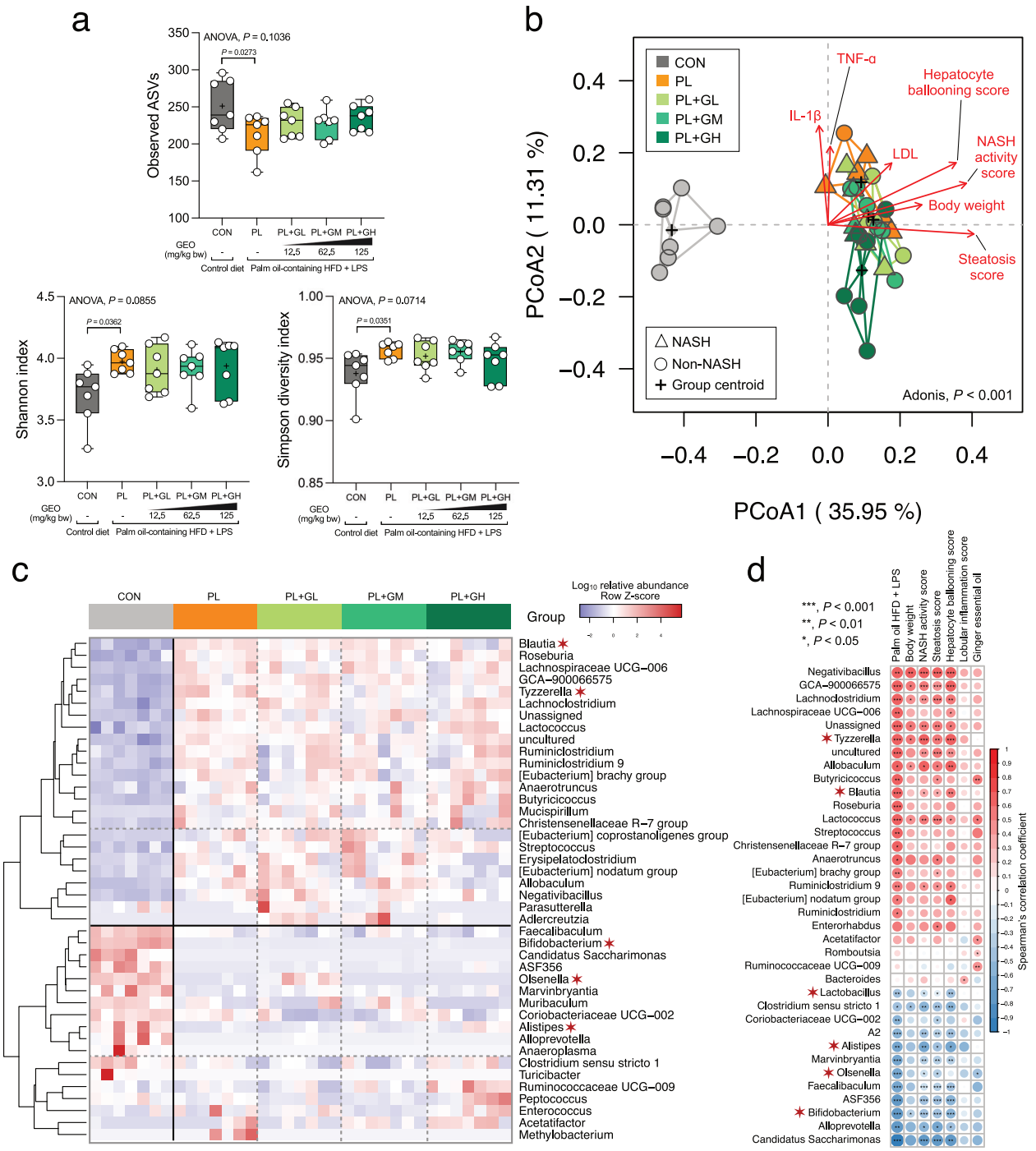

Fig. 5 PL and GEO remodel the composition of fecal microbiota. a α-diversity indices, observed ASVs, Shannon index, and Simpson diversity index, **b** principal coordinate analysis (PCoA) plot based on Bray–Curtis dissimilarity with biomarker vector, **c** heatmap of the relative abundances at genera level, and **d** Spearman's correlation analysis between gut microbiota components and NASH-related parameters in C57BL/6 mice, which were treated with either control or a palm oil-containing HFD with LPS i.p. (PL) with or without ginger essential oil (GEO) (12.5 (GL), 62.5 (GM), and 125 (GH) mg/kg bw) supplementation by daily oral gavage for 12 weeks. Each value was expressed as the mean ± SD ($n = 7$). Statistical analyses were performed by a one-way ANOVA with Dunnett's multiple comparison test for comparing group means against the PL group. Analysis of variance using distance matrices (Adonis) were calculated to determine the heterogeneity of the feces microbiota among the groups in PCoA. Vectors in the PCoA plot indicated a significant effect of biomarkers ($p < 0.05$), and its length shows the strength of the correlation.

increased (Fig. 5a). GEO did not cause a shift in α-diversity. The β-diversity based on the Bray−Curtis distance (PC1: 35.95% and PC2: 11.31%) demonstrated that both PL intervention and GEO significantly impact gut microbiota remodeling (Adonis, $p < 0.001$). PL intervention was a primary factor in the shift in the gut microbiota in PCoA1 (Fig. 5b). GEO further played a secondary role in gut microbiota remodeling in a dose-dependent manner in PCoA2. Among the GEO-treated groups, the gut microbiota

shifted from that of the PL group in a dose-dependent manner. A high dose of GEO (PL + GH group) shifted outward from the PL group, suggesting that a higher dosage of GEO exhibits a more substantial effect on gut microbiota remodeling. We further assessed the association between NASH-related features and gut microbiota composition using the envfit function of the vegan R package. The results are shown in Fig. 5b as red vectors. The direction of the vectors from the centroid was opposite to that of the control group and encountered NASH-phenotype mice. NASH- and obesity-related parameters exhibited a significant association with the gut microbiota of NASH mice ($p < 0.05$), including NASH activity scores, hepatocyte ballooning, steatosis scores, body weights, LDLs, TNF-α, and IL-1β. The heatmap showed 42 different significant genera based on the Kruskal–Wallis test with an FDR-adjusted p-value ($p < 0.05$), as presented in Fig. 5c. Heatmap hierarchical clustering displayed two main clusters, indicating that PL intervention was the main factor that altered the gut microbiota at the genus level. Spearman's correlation analysis was then performed to assess NASH and obesity biomarkers. The results demonstrated that 16 genera were positively correlated with NASH and obesity biomarkers; conversely, 12 genera were negatively correlated (Fig. 5d). Among them, the NASH-related microbiota, including *Tyzzerella* and *Blautia*, showed a positive correlation. In contrast, beneficial bacteria, such as *Lactobacillus*, *Alistipes*, *Olsenella*, and *Bifidobacterium*, exhibited a negative correlation. However, the correlation between GEO and NASH-related microbiota was reduced, suggesting that GEO supplementation may protect against the dysbiosis of gut microbiota. The NASH-related microbiota, including *Blautia* and *Tyzzerella*, trended to be suppressed by GEO, especially at high doses ($p = 0.1216$ and $p. = 0.0756$, respectively) (Supplementary Fig. 4a, b). Beneficial genera, including *Alitipes*, *Bifidobacterium*, *Lactobacillus*, and *Olsenella*, were depleted in the PL group. GEO at a high dose trended to recover *Alistpes* and *Lactobacillus*, and the low dose resulted in the enrichment of *Olsenella* (Supplementary Fig. 4c–f). GEO supplementation in PL may therefore reverse gut microbiota dysbiosis and ameliorate NASH.

GEO alleviates NASH by modulating the LPS/TLR4/NF-κB signaling pathway

Unhealthy diets, low in fiber and high in fat and sugar, can lead to gut microbiota dysbiosis and intestinal barrier leakage. This compromised barrier facilitates the translocation of gut microbiota-derived metabolites, such as LPS, into the liver [13, 14]. GEO resulted in favorable gut microbiota remodeling, as described in the previous section. To understand the beneficial effect of GEO on intestinal permeability, we administered fluorescein isothiocyanate (FITC)-dextran to the mice and detected the fluorescence intensity in the plasma. PL trended to increase the fluorescence intensity in the plasma, suggesting that PL intervention results in intestinal leakage. GEO supplementation trended to reduce intestinal permeability (Fig. 6a). The dysfunction of the intestinal barrier allows gut microbial LPS to enter the liver and circulatory system through the portal vein and lymphatic system, thereby promoting inflammation. The murine TLR4/NF-κB/SEAP reporter HEK293 cell assay was used to detect LPS levels. The results demonstrated no significant differences in plasma LPS levels among the control, PL-, and GEO-treated groups (Fig. 6b). Interestingly, hepatic LPS levels were markedly elevated ($p < 0.0001$) compared to those in the CON group. GEO supplementation in PL intervention at low, medium, and high doses significantly reduced hepatic LPS levels ($p < 0.0001$, $p = 0.0001$, and $p < 0.0001$, respectively) (Fig. 6c). Mechanistically, gut-derived LPS activated the TLR4/NF-κB pathway and triggered hepatic inflammation. We further examined the hepatic protein expression of TLR4 and NF-κB. Both hepatic TLR4 and NF-κB levels were higher in the PL group than in the CON group ($p = 0.0141$ and $p = 0.0022$, respectively) (Fig. 6d, e). Low, medium, and high doses of GEO trended to reduced TLR4 ($p = 0.1142$, $p = 0.0448$, and $p = 0.0029$, respectively) and NF-κB protein expression ($p = 0.0053$, $p = 0.0025$, and $p < 0.0001$, respectively) (Fig. 6e, f), thereby resulting in the reduction of the pro-inflammatory cytokines TNF-α, IL-1β, and IL-6, and the NAS (Fig. 4a–c and Fig. 2e). Collectively, these results demonstrate the potential protective effect of GEO against NASH via modulating the gut microbiota and its metabolite–liver axis through the LPS/TLR4/NF-κB signaling pathway.

DISCUSSION

A trans-fat-containing HFD is an excellent model for inducing NASH in animals [24]. Due to the prohibition of using trans-fats in the food supply chain and food industry [23], however, trans-fat-containing HFDs may not be suitable for mimicking NASH progression in humans. The replacement of trans-fat with palm oil in a HFD exhibits advantages and the potential for inducing NASH with human NASH phenotype translatability [25]. P-HFD-fed rodents manifest morphological features analogous to those of human NASH, including macrosteatosis, lobular inflammation, hepatocyte ballooning degeneration, and periportal/perisinusoidal fibrosis [25]. Furthermore, we developed a P-HFD supplemented with an intraperitoneal injection of LPS (PL) to mimic the conditions of gut dysbiosis and endotoxemia. PL causes NASH, intestinal leakage, endotoxemia, and dysbiosis of the intestinal microbiota by increasing pathogenic bacteria and reducing beneficial microbiota [26]. Therefore, a PL mouse model was used in this study. Our results demonstrated that PL intervention for 12 weeks negatively affected obesogenic and metabolic biomarkers in mice, including body weight, the area under the curve (AUC) of body weight gain, total fat mass, plasma glucose, total cholesterol, and LDL-C (Fig. 1). The average energy intake of the mice among the groups was not significantly different, suggesting that the adverse obesogenic and metabolic consequences were due to the P-HFDs and LPS injections. The P-HFD diet comprised a large amount of palm oil, fat, fructose, and cholesterol. A previous study found that dietary saturated fat and fructose intake are associated with intrahepatic lipid accumulation, lipogenesis, insulin resistance, oxidative stress, and inflammation [38, 39]. Palm oil contains a large amount of saturated fatty palmitic acid (C16:0) [40]. Palm oil in normocaloric and normolipidic diets can adversely interfere with and exacerbate metabolic and glucose homeostasis and induce inflammation in the liver and white adipose tissue. The consequence is more acute in mice administered interesterified palm oil [41]. Injections of LPS in choline-deficient l-amino-acid-defined (CDAA)-fed mice for 16 weeks have been found to intensify hepatic inflammation and pericellular fibrosis via the TLR4/NF-κB signaling pathway [42]. This study demonstrated that the use of PL could be more advantageous than the CDAA diet as PL can mimic the human diet and endotoxemia, whereas the CDAA diet is not practical in humans. In this study, the level of plasma TG declined in the PL group compared to the CON group, which is consistent with previous studies [24, 25] and was likely due to blood cholesterol in the P-HFD inhibiting lipoprotein synthesis, thereby reducing triglyceride secretion from the liver to the circulation [43, 44]. In this study, GEO supplementation prevented the obesogenic metabolic phenotype and ameliorated lipidemia by reducing the body weight and plasma glucose, total triglycerides, and LDL-C, and by increasing HDL-C. GEO further alleviated the NASH phenotype by attenuating the plasma hepatic damage biomarkers AST, ALT, and NAS, mainly by reducing the hepatocyte ballooning score. Hepatocyte ballooning is generally considered to be a form of apoptosis related to fibrosis and cytoskeletal damage [45]. In this study, medium and high doses of GEO (62.5 and 125 mg/kg bw) exhibited a more substantial hepatoprotective effect. GEO displays an anti-hyperlipidemic effect by reducing serum FFA, triglycerides, and total cholesterol

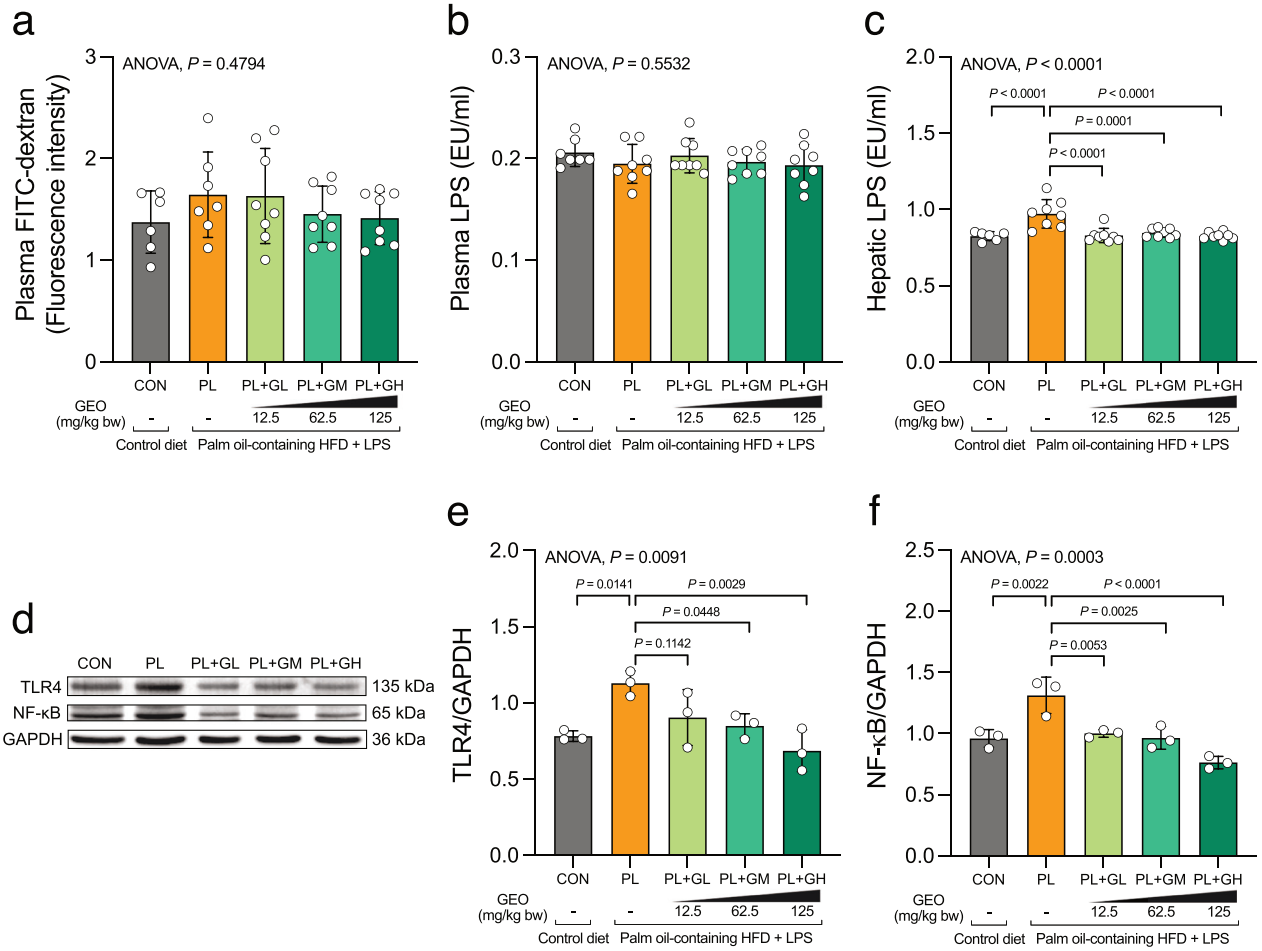

Fig. 6 GEO reduces liver inflammation by suppressing the gut-derived LPS/TLR4/NF-κB signaling pathway. a Intestinal permeability based on plasma FITC-dextran intensity, **b** plasma LPS, **c** hepatic LPS, **d** representative image of TLR4 and NF-κB protein expression, **e** TLR4 protein expression, and **f** NF-κB protein expression in C57BL/6 mice, which were treated with either control or a palm oil-containing HFD with LPS i.p. (PL) with or without ginger essential oil (GEO) (12.5 (GL), 62.5 (GM), and 125 (GH) mg/kg bw) supplementation by daily oral gavage for 12 weeks. Each value was expressed as the mean ± SD ($n = 7–8$), protein expression ($n = 3$). Statistical analyses were performed by a one-way ANOVA with Dunnett's multiple comparison test for comparing group means against the PL group.

levels in mice, previously reported [6]. GEO exhibits hepatoprotective properties against alcoholic fatty liver disease and can change particular metabolites in the blood [32].

HFD intake is associated with increased oxidative stress in the liver, which is one of the pathogeneses of NASH [46]. NASH patients have been found to exhibit increased CYP2E1, which promotes ROS generation and hepatic oxidative stress [47]. Several studies have further demonstrated that ginger exerts antioxidant activity [6, 32, 48]. In this study, GEO supplementation trended to lower hepatic CYP2E1 protein expression and significantly enhanced the hepatic antioxidant enzyme capacity, including CAT, GRd, and GSH. These results demonstrate that GEO alleviates hepatic oxidative stress in mice with PL-induced NASH. HFD consumption interferes with homeostasis by impairing lipid metabolism, resulting in imbalanced lipid uptake and storage and leading to hepatic steatosis [7, 49]. The PL-induced NASH mouse group showed a trended to increase in the hepatic protein expression of SREBP-1 and HMGCR compared to the control mice. Both of these transcription factors play essential roles in the regulation of hepatic lipid biosynthesis. The elevation of SREBP-1c promotes triglyceride synthesis, and HMGCR is a key enzyme in cholesterol synthesis [50]. In addition, PPARα, a regulator of fatty acid β-oxidation, decreased in PL-induced NASH mice. The effect of GEO on these lipid-regulating proteins exhibited a substantial improve, but it did not reach statistical significance, which was consistent with the histopathological data. The different forms of diet-induced NASH models could induce different degrees of NASH severity. PL-induced NASH showed substantial severity compared to our previous study, in which HFD induced simple hepatic steatosis [6, 51].

GEO alleviated the NASH phenotype and pro-inflammatory cytokines TNF-α, IL-6, and IL-1β. Therefore, we investigated the underlying mechanisms of inflammation. The NLRP3 inflammasome plays an essential role in the hepatic inflammatory response [52]. NASH patients and animal models have exhibited increases in the activation of the NLRP3 inflammasome [17, 52]. Blocking the NLRP3 inflammasome attenuates hepatic steatosis, inflammation, and fibrosis in mice [17]. In our study, the expression levels of NLRP3 and ASC were increased in PL-induced mice, whereas they were reduced with GEO supplementation. Caspase-1 protein expression was trended to suppressed by GEO. The activation of the NLRP3 inflammasome is stimulated by danger-associated molecular patterns and PAMPs such as LPS [53]. The LPS-mediated TLR4/NF-κB pathway can activate the NLRP3 inflammasome by enhancing the expression of NLRP3 [54]. In in vitro experiments, geranial and neral isomers of citral in GEO suppressed the production of the NLRP3 inflammasome and pro-IL-1β [55]. Therefore, GEO exhibited anti-inflammatory activity by reducing

NLRP3 inflammasome activation, which may be caused by citral and its isomers.

Diet is a primary factor in modifying the composition of gut microbiota [56]. PL intervention is a prime factor in modifying the fecal microbiota composition of mice. GEO has less influence on α-diversity. Similarly, PCoA β-diversity based revealed that diet is the principal factor that shapes the gut microbiota. GEO plays a secondary role in modifying gut microbiota bacterial diversity. A high dose of GEO resulted in the gut microbiota shifting outward from the PL-treated group. GEO reduced the relative abundance of NASH-associated bacteria, including *Blautia* and *Tyzzerella*, which are considered potentially harmful. Compared to healthy individuals, *Blautia* abundance increased in NASH patients and was positively correlated with LPS levels [57]. *Tyzzerella* has been reported to be enriched after 12 weeks of HFD intervention and is positively associated with liver dysfunction-associated parameters [58]. In contrast, GEO supplementation in PL mice enhanced the relative abundance of *Lactobacillus*, *Alistipes*, and *Olsenella*, which are considered beneficial bacteria. A previous study reported a lower relative abundance of *Lactobacillus* in GAN *ob/ob*-NASH mice [24]. *Lactobacillus* may be used as a probiotic to improve steatohepatitis through the gut microbiota–liver axis by modulating gut microbiota composition and the inflammatory pathway in NAFLD [59]. *Alistipes*, which are potential SCFA-producing bacteria that reduce hepatic fibrotic conditions through cytokine modulation, have been found at lower levels in the guts of NASH and NASH-cirrhosis patients [60, 61]. *Olsenella*, an SCFA producer, is associated with tight junction improvement [62, 63]. Thus, GEO supplementation can remodel gut microbiota composition and reverse gut microbiota dysbiosis, which may contribute to ameliorating NASH. This study has a limitation in that all mice for each treatment were housed in separate cages, and the mice did not receive the same microbiomes from the start. Given that mice are coprophagic, this may introduce a potential cage effect. To mitigate these confounding factors, future studies should consider co-housing the mice and ensuring they receive the same microbiomes from the beginning. This approach would allow for a more precise assessment of the effects of diet and dietary supplements on the gut microbiota.

The elevated localization of LPS in hepatocytes has been reported in NAFLD and may cause liver inflammation via a TLR4-related pathway [64]. This study found no significant changes in intestinal permeability or plasma LPS levels in PL-induced mice, whereas hepatic LPS levels were noted to increase. Although we observed increased intestinal permeability of PL mice, the lack of statistical significance may be due to individual variations in gut permeability within the PL group. Based on our experimental design, we administered P-HFD mice with weekly intraperitoneal injections of LPS. The low-dose, weekly intraperitoneal injection of LPS in our study is unlikely to have substantially affected plasma and hepatic LPS levels, as the observed levels were relatively low compared to the injection dose. Additionally, LPS in the circulation was found at a level similar to that in the control group, these data suggested that the elevation of hepatic LPS levels in the liver was derived from the gut and not the extra injection of LPS. LPS is a risk factor for inducing hepatic inflammation and NASH. The upregulation of the LPS-TLR4 pathway leads to NF-κB activation and inflammatory cytokine production, which play key roles in NASH progression and development [42]. PL-induced NASH mice exhibited a higher expression of TLR4 and NF-κB, which resulted in a more severe inflammatory condition than mice supplemented with GEO. In addition to the TLR4/NF-κB pathway, LPS is also involved in activating the NLRP3 inflammasome [65].

We also conducted a dosage translation of GEO from mice to humans and compared it with the dosage achievable from natural ginger (Supplementary Fig. 5). Our analysis indicates that the dosage used in the study can be obtained from natural ginger, suggesting the potential development of GEO as a functional food or food supplement. Nevertheless, further investigation through human studies is required to comprehensively evaluate its potential applications. Histological analysis of kidney, spleen, and ileum sections in the GEO-treated group did not reveal any significant findings, as shown in Supplementary Fig. 6. These results indicate the safety of GEO under our experimental conditions. Moreover, a subchronic toxicity study conducted on Wistar rats for a duration of 13 weeks reported no observed adverse effect level (NOAEL) of 500 mg/kg body weight [66]. When extrapolated to mouse dosage [67], this corresponds to 1000 mg/kg body weight. Importantly, it should be noted that the dosages utilized in our study were relatively lower than the NOAEL reported in the literature, providing further evidence of the safety profile of GEO at the selected dosages.

Collectively, the results of our study demonstrated that GEO exhibits a potential hepatoprotective effect by preventing NASH progression in a PL-induced NASH mouse model. The mechanisms of action of GEO may include reducing liver steatosis and oxidative stress, blocking the NLRP3 inflammasome pathway, and remodeling the LPS/TLR4/NF-κB pathway which could be modulated by changes in gut microbiota. GEO, therefore, may be used as a dietary supplement to prevent NASH.

DATA AVAILABILITY

The raw 16 s rRNA sequencing data used to produce all figures are accessible in the NCBI Short Read Archive under the following accession numbers: BioProject (PRJNA854318), BioSample (SAMN29428094), and SRA (SRR19905849-83).

CODE AVAILABILITY

Bioinformatic tools, software version, parameters, and open-source code used in this present study are described in the "Methods" section. More details regarding the code to reproduce the analyses are available upon request.

REFERENCES

1. Younossi Z, Anstee QM, Marietti M, Hardy T, Henry L, Eslam M, et al. Global burden of NAFLD and NASH: trends, predictions, risk factors and prevention. Nat Rev Gastroenterol Hepatol. 2018;15:11–20.
2. Brunt EM, Wong VW, Nobili V, Day CP, Sookoian S, Maher JJ, et al. Nonalcoholic fatty liver disease. Nat Rev Dis Primers. 2015;1:15080.
3. Aron-Wisnewsky J, Vigliotti C, Witjes J, Le P, Holleboom AG, Verheij J, et al. Gut microbiota and human NAFLD: disentangling microbial signatures from metabolic disorders. Nat Rev Gastroenterol Hepatol. 2020;17:279–97.
4. Buzzetti E, Pinzani M, Tsochatzis EA. The multiple-hit pathogenesis of non-alcoholic fatty liver disease (NAFLD). Metabolism. 2016;65:1038–48.
5. Arroyave-Ospina JC, Wu ZM, Geng YN, Moshage H. Role of oxidative stress in the pathogenesis of non-alcoholic fatty liver disease: Implications for prevention and therapy. Antioxidants. 2021;10:174.
6. Lai YS, Lee WC, Lin YE, Ho CT, Lu KH, Lin SH, et al. Ginger Essential oil ameliorates hepatic injury and lipid accumulation in high fat diet-induced nonalcoholic fatty liver disease. J Agric Food Chem. 2016;64:2062–71.
7. Ipsen DH, Lykkesfeldt J, Tveden-Nyborg P. Molecular mechanisms of hepatic lipid accumulation in non-alcoholic fatty liver disease. Cell Mol Life Sci. 2018;75:3313–27.
8. Han KH, Hashimoto N, Fukushima M. Relationships among alcoholic liver disease, antioxidants, and antioxidant enzymes. World J Gastroentero. 2016;22:37–49.
9. Swanson KV, Deng M, Ting JP. The NLRP3 inflammasome: molecular activation and regulation to therapeutics. Nat Rev Immunol. 2019;19:477–89.
10. Vandanmagsar B, Youm YH, Ravussin A, Galgani JE, Stadler K, Mynatt RL, et al. The NLRP3 inflammasome instigates obesity-induced inflammation and insulin resistance. Nat Med. 2011;17:179–88.
11. Gentile CL, Weir TL. The gut microbiota at the intersection of diet and human health. Science. 2018;362:776–80.

12. Jennison E, Byrne CD. The role of the gut microbiome and diet in the pathogenesis of non-alcoholic fatty liver disease. Clin Mol Hepatol. 2021;27:22–43.
13. Hrncir T, Hrncirova L, Kverka M, Hromadka R, Machova V, Trckova E, et al. Gut microbiota and NAFLD: pathogenetic mechanisms, microbiota signatures, and therapeutic interventions. Microorganisms. 2021;9:957.
14. Albillos A, de Gottardi A, Rescigno M. The gut-liver axis in liver disease: Pathophysiological basis for therapy. J Hepatol. 2020;72:558–77.
15. Dapito DH, Mencin A, Gwak GY, Pradere JP, Jang MK, Mederacke I, et al. Promotion of hepatocellular carcinoma by the intestinal microbiota and TLR4. Cancer Cell. 2012;21:504–16.
16. Kolodziejczyk AA, Zheng DP, Shibolet O, Elinav E. The role of the microbiome in NAFLD and NASH. Embo Mol Med. 2019;11:e9302.
17. Wree A, McGeough MD, Pena CA, Schlattjan M, Li HY, Inzaugarat ME, et al. NLRP3 inflammasome activation is required for fibrosis development in NAFLD. J Mol Med. 2014;92:1069–82.
18. Ikawa-Yoshida A, Matsuo S, Kato A, Ohmori Y, Higashida A, Kaneko E, et al. Hepatocellular carcinoma in a mouse model fed a choline-deficient, L-amino acid-defined, high-fat diet. Int J Exp Pathol. 2017;98:221–33.
19. Mu YP, Ogawa T, Kawada N. Reversibility of fibrosis, inflammation, and endoplasmic reticulum stress in the liver of rats fed a methionine-choline-deficient diet. Lab Invest. 2010;90:245–56.
20. Clapper JR, Hendricks MD, Gu G, Wittmer C, Dolman CS, Herich J, et al. Diet-induced mouse model of fatty liver disease and nonalcoholic steatohepatitis reflecting clinical disease progression and methods of assessment. Am J Physiol Gastrointest Liver Physiol. 2013;305:G483–95.
21. Brownell KD, Pomeranz JL. The trans-fat ban-food regulation and long-term health. N Engl J Med. 2014;370:1773–5.
22. Grossman MR. USA: FDA issues order to ban artificial trans fat by 2018 reports. Eur Food Feed L Rev. 2015;10:317.
23. Parziale A, Ooms G. The global fight against trans-fat: the potential role of international trade and law. Global Health. 2019;15:46.
24. Boland ML, Oro D, Tolbol KS, Thrane ST, Nielsen JC, Cohen TS, et al. Towards a standard diet-induced and biopsy-confirmed mouse model of non-alcoholic steatohepatitis: impact of dietary fat source. World J Gastroenterol. 2019;25:4904–20.
25. Hansen HH, Ægidius HM, Oro D, Evers SS, Heeboll S, Eriksen PL, et al. Human translatability of the GAN diet-induced obese mouse model of non-alcoholic steatohepatitis. BMC Gastroenterol. 2020;20:210.
26. Sheen LY, Panyod S, Wu WK, Hsieh YC, Tseng YJ, Peng SY, et al. Establishment of animal models for NASH and utilization for mining associated gut microbiota. Res Sq. 2022. https://doi.org/10.21203/rs.3.rs-1826044/v1.
27. Pappachan JM, Babu S, Krishnan B, Ravindran NC. Non-alcoholic fatty liver disease: a clinical update. J Clin Transl Hepatol. 2017;5:384–93.
28. Ganesan K, Jayachandran M, Xu B. A critical review on hepatoprotective effects of bioactive food components. Crit Rev Food Sci Nutr. 2018;58:1165–229.
29. Wang X, Shen Y, Thakur K, Han J, Zhang JG, Hu F, et al. Antibacterial activity and mechanism of ginger essential oil against *Escherichia coli* and *Staphylococcus aureus*. Molecules. 2020;25:3955.
30. Nerilo SB, Rocha GHO, Tomoike C, Mossini SAG, Grespan R, Mikcha JMG, et al. Antifungal properties and inhibitory effects upon aflatoxin production by Zingiber officinale essential oil in Aspergillus flavus. Int J Food Sci Tech. 2016;51:286–92.
31. Panyod S, Wu WK, Peng SY, Tseng YJ, Hsieh YC, Chen RA, et al. Ginger essential oil and citral ameliorates atherosclerosis in ApoE$^{-/-}$ mice by modulating trimethylamine-N-oxide and gut microbiota. NPJ Sci Food. 2023;7:19.
32. Liu CT, Raghu R, Lin SH, Wang SY, Kuo CH, Tseng YJ, et al. Metabolomics of ginger essential oil against alcoholic fatty liver in mice. J Agric Food Chem. 2013;61:11231–40.
33. Liang W, Menke AL, Driessen A, Koek GH, Lindeman JH, Stoop R, et al. Establishment of a general NAFLD scoring system for rodent models and comparison to human liver pathology. PLoS ONE. 2014;9:e115922.
34. Panyod S, Wu WK, Ho CT, Lu KH, Liu CT, Chu YL, et al. Diet supplementation with allicin protects against alcoholic fatty liver disease in mice by improving anti-inflammation and antioxidative functions. J Agric Food Chem. 2016;64:7104–13.
35. Bolyen E, Rideout JR, Dillon MR, Bokulich NA, Abnet CC, Al-Ghalith GA, et al. Reproducible, interactive, scalable and extensible microbiome data science using QIIME 2 (vol 37, pg 852, 2019). Nat Biotechnol. 2019;37:1091.
36. Chassaing B, Koren O, Goodrich JK, Poole AC, Srinivasan S, Ley RE, et al. Dietary emulsifiers impact the mouse gut microbiota promoting colitis and metabolic syndrome. Nature. 2015;519:92–6.
37. Nobili V, Pastore A, Gaeta LM, Tozzi G, Comparcola D, Sartorelli MR, et al. Glutathione metabolism and antioxidant enzymes in patients affected by nonalcoholic steatohepatitis. Clin Chim Acta. 2005;355:105–11.
38. Lim JS, Mietus-Snyder M, Valente A, Schwarz JM, Lustig RH. The role of fructose in the pathogenesis of NAFLD and the metabolic syndrome. Nat Rev Gastro Hepat. 2010;7:251–64.
39. Meex RCR, Blaak EE. Mitochondrial dysfunction is a key pathway that links saturated fat intake to the development and progression of NAFLD. Mol Nutr Food Res. 2021;65:e1900942.
40. Montoya C, Cochard B, Flori A, Cros D, Lopes R, Cuellar T, et al. Genetic architecture of palm oil fatty acid composition in cultivated oil palm (*Elaeis guineensis* Jacq.) compared to its wild relative E. Oleifera (HBK) Cortes. PLoS ONE. 2014;9:e95412.
41. Miyamoto JE, Reginato A, Portovedo M, dos Santos RM, Stahl MA, Le Stunff H, et al. Interesterified palm oil impairs glucose homeostasis and induces deleterious effects in liver of Swiss mice. Metab Clin Exp. 2020;112:154350.
42. Nakanishi K, Kaji K, Kitade M, Kubo T, Furukawa M, Saikawa S, et al. Exogenous administration of low-dose lipopolysaccharide potentiates liver fibrosis in a choline-deficient l-amino-acid-defined diet-induced murine steatohepatitis model. Int J Mol Sci. 2019;20:2724.
43. Ma K, Malhotra P, Soni V, Hedroug O, Annaba F, Dudeja A, et al. Overactivation of intestinal SREBP2 in mice increases serum cholesterol. PLoS ONE. 2014;9:e84221.
44. Henkel J, Coleman CD, Schraplau A, Jhrens K, Weber D, Castro JP, et al. Induction of steatohepatitis (NASH) with insulin resistance in wildtype B6 mice by a western-type diet containing soybean oil and cholesterol. Mol Med. 2017;23:70–82.
45. Caldwell S, Ikura Y, Dias D, Isomoto K, Yabu A, Moskaluk C, et al. Hepatocellular ballooning in NASH. J Hepatol. 2010;53:719–23.
46. Dhibi M, Brahmi F, Mnari A, Houas Z, Chargui I, Bchir L, et al. The intake of high fat diet with different trans fatty acid levels differentially induces oxidative stress and non alcoholic fatty liver disease (NAFLD) in rats. Nutr Metab. 2011;8:65.
47. Aubert J, Begriche K, Knockaert L, Robin MA, Fromenty B. Increased expression of cytochrome P450 2E1 in nonalcoholic fatty liver disease: mechanisms and pathophysiological role. Clin Res Hepatol Gastroenterol. 2011;35:630–7.
48. Stoilova I, Krastanov A, Stoyanova A, Denev P, Gargova S. Antioxidant activity of a ginger extract (Zingiber officinale). Food Chem. 2007;102:764–70.
49. Chen Z, Tian R, She Z, Cai J, Li H. Role of oxidative stress in the pathogenesis of nonalcoholic fatty liver disease. Free Radic Biol Med. 2020;152:116–41.
50. Sekiya M, Yahagi N, Matsuzaka T, Takeuchi Y, Nakagawa Y, Takahashi H, et al. SREBP-1-independent regulation of lipogenic gene expression in adipocytes. J Lipid Res. 2007;48:1581–91.
51. Lai YS, Chen WC, Ho CT, Lu KH, Lin SH, Tseng HC, et al. Garlic essential oil protects against obesity-triggered nonalcoholic fatty liver disease through modulation of lipid metabolism and oxidative stress. J Agric Food Chem. 2014;62:5897–906.
52. Thomas H. NAFLD: A critical role for the NLRP3 inflammasome in NASH. Nat Rev Gastroenterol Hepatol. 2017;14:197.
53. Gong T, Liu L, Jiang W, Zhou R. DAMP-sensing receptors in sterile inflammation and inflammatory diseases. Nat Rev Immunol. 2020;20:95–112.
54. Guo H, Callaway JB, Ting JP. Inflammasomes: mechanism of action, role in disease, and therapeutics. Nat Med. 2015;21:677–87.
55. Liao PC, Yang TS, Chou JC, Chen J, Lee SC, Kuo YH, et al. Anti-inflammatory activity of neral and geranial isolated from fruits of *Litsea cubeba* Lour. J Funct Foods. 2015;19:248–58.
56. Leeming ER, Johnson AJ, Spector TD, Le Roy CI. Effect of diet on the gut microbiota: Rethinking intervention duration. Nutrients. 2019;11:2862.
57. Del Chierico F, Nobili V, Vernocchi P, Russo A, De Stefanis C, Gnani D, et al. Gut microbiota profiling of pediatric nonalcoholic fatty liver disease and obese patients unveiled by an integrated meta-omics-based approach. Hepatology. 2017;65:451–64.
58. Li RJ, Jie ZY, Feng Q, Fang RL, Li F, Gao Y, et al. Network of interactions between gut microbiome, host biomarkers, and urine metabolome in carotid atherosclerosis. Front Cell Infect Mi. 2021;11:708088.
59. Lee NY, Yoon SJ, Han DH, Gupta H, Youn GS, Shin MJ, et al. *Lactobacillus* and *Pediococcus* ameliorate progression of non-alcoholic fatty liver disease through modulation of the gut microbiome. Gut Microbes. 2020;11:882–99.
60. Astbury S, Atallah E, Vijay A, Aithal GP, Grove JI, Valdes AM. Lower gut microbiome diversity and higher abundance of proinflammatory genus *Collinsella* are associated with biopsy-proven nonalcoholic steatohepatitis. Gut Microbes. 2020;11:569–80.
61. Parker BJ, Wearsch PA, Veloo ACM, Rodriguez-Palacios A. The genus *Alistipes*: Gut bacteria with emerging implications to inflammation, cancer, and mental health. Front Immunol. 2020;11:906.
62. Du F, Huang RF, Lin D, Wang YY, Yang XH, Huang XY, et al. Resveratrol improves liver steatosis and insulin resistance in non-alcoholic fatty liver disease in association with the gut microbiota. Front Microbiol. 2021;12:611323.
63. Li W, Zhang K, Yang H. Pectin alleviates high fat (lard) diet-induced nonalcoholic fatty liver disease in mice: Possible role of short-chain fatty acids and gut microbiota regulated by pectin. J Agric Food Chem. 2018;66:8015–25.

64. Carpino G, Del Ben M, Pastori D, Carnevale R, Baratta F, Overi D, et al. Increased liver localization of lipopolysaccharides in human and experimental NAFLD. Hepatology. 2020;72:470–85.
65. Fusco R, Siracusa R, Genovese T, Cuzzocrea S, Di Paola R. Focus on the role of NLRP3 inflammasome in diseases. Int J Mol Sci. 2020;21:4223.
66. Jeena K, Liju VB, Kuttan R. A preliminary 13-week oral toxicity study of ginger oil in male and female Wistar rats. Int J Toxicol. 2011;30:662–70.
67. Reagan-Shaw S, Nihal M, Ahmad N. Dose translation from animal to human studies revisited. FASEB J. 2008;22:659–61.

ACKNOWLEDGEMENTS

This study was financed by the Ministry of Science and Technology (Taiwan) (109-2327-B-002-005, 109-2314-B-002-103-MY3, 109-2314-B-002-064-MY3, 110-2327-B-002-007, 111-2628-B-002-047, and 111-2327-B-002-008) and the National Science and Technology Council, Taiwan (NSTC 112-2327-B-002-009, 113-2321-B-002-026, and 113-2321-B-002-022). The authors acknowledge the research collaboration and technical support provided by the National Human Microbiome Core Facility, Taiwan (NSTC 112-2740-B-A49-002 and 113-2740-B-A49-003).

AUTHOR CONTRIBUTIONS

SP designed, instructed and assisted the experiment, performed the bioinformatics and statistical analysis, and drafted the manuscript; WKW instructed the experiments and reviewed the manuscript; YCH, YJT, SYP performed the animal experiments; RAC and HSH assisted animal experiment; YHC assisted animal and LPS quantification experiment; TCDS, CTH, CJL, HLC, and CCH critically reviewed the manuscript; MSW and LYS designed the experiments, provided the funding for the study, and critically revised the manuscript.

COMPETING INTERESTS

The authors declare no competing interests.

ETHICS APPROVAL AND CONSENT TO PARTICIPATE

Animal experiments were approved by the Institutional Animal Care and Use Committee of National Taiwan University (IACUC) (Approval No: NTU-110-EL-00060).

ADDITIONAL INFORMATION

Supplementary information The online version contains supplementary material available at https://doi.org/10.1038/s41387-024-00306-1.

Correspondence and requests for materials should be addressed to Ming-Shiang Wu or Lee-Yan Sheen.

Reprints and permission information is available at http://www.nature.com/reprints

Publisher's note Springer Nature remains neutral with regard to jurisdictional claims in published maps and institutional affiliations.